AGU PUBLICATIONS

Geophysical Research Letters

RESEARCH LETTER
10.1002/2016GL069314

Special Section:
The Arctic: An AGU Joint Special Collection

Using timing of ice retreat to predict timing of fall freeze-up in the Arctic

Julienne C. Stroeve[1,2], Alex D. Crawford[1], and Sharon Stammerjohn[3]

[1]National Snow and Ice Data Center, Cooperative Institute for Research in Environmental Sciences, University of Colorado Boulder, Boulder, Colorado, USA, [2]Centre for Polar Observation and Modelling, University College London, London, UK, [3]Institute for Arctic and Alpine Research, Cooperative Institute for Research in Environmental Sciences, University of Colorado Boulder, Boulder, Colorado, USA

Abstract Reliable forecasts of the timing of sea ice advance are needed in order to reduce risks associated with operating in the Arctic as well as planning of human and environmental emergencies. This study investigates the use of a simple statistical model relating the timing of ice retreat to the timing of ice advance, taking advantage of the inherent predictive power supplied by the seasonal ice-albedo feedback and ocean heat uptake. Results show that using the last retreat date to predict the first advance date is applicable in some regions, such as Baffin Bay and the Laptev and East Siberian seas, where a predictive skill is found even after accounting for the long-term trend in both variables. Elsewhere, in the Arctic, there is some predictive skills depending on the year (e.g., Kara and Beaufort seas), but none in regions such as the Barents and Bering seas or the Sea of Okhotsk. While there is some suggestion that the relationship is strengthening over time, this may reflect that higher correlations are expected during periods when the underlying trend is strong.

Key Points:
- Statistical model relates timing of sea ice retreat to timing of ice advance in the Arctic
- Highlights regions of Arctic where ice-albedo dominates
- Modest skill is found in Baffin Bay, Laptev, and East Siberian seas

Supporting Information:
- Supporting Information S1

Correspondence to:
J. C. Stroeve,
stroeve@colorado.edu

Citation:
Stroeve, J. C., A. D. Crawford, and S. Stammerjohn (2016), Using timing of ice retreat to predict timing of fall freeze-up in the Arctic, *Geophys. Res. Lett.*, *43*, 6332–6340, doi:10.1002/2016GL069314.

Received 1 MAY 2016
Accepted 25 MAY 2016
Accepted article online 4 JUN 2016
Published online 20 JUN 2016

1. Introduction

The Arctic is experiencing profound sea ice declines, with the nine lowest September sea ice extents (SIEs) occurring in the last 9 years [*Simmonds*, 2015; *Serreze and Stroeve*, 2015]. While negative anomalies are seen in all months (Figure S1 in the supporting information), they are most pronounced during summer, leading to longer open water periods (OWPs) and more accessibility. Since 1979, the duration of the OWP has lengthened by about a week each decade, dominated by later autumn freeze-up with smaller trends toward earlier melt onset [*Stroeve et al.*, 2014a]. Later freeze-up dominates the trend because ocean mixed-layer temperatures are increased by increased absorption of solar radiation in the open water areas [*Steele et al.*, 2008; *Stammerjohn et al.*, 2012; *Stroeve et al.*, 2012; *Perovich et al.*, 2007].

The lengthening of the OWP has evoked increased interest in marine activity and resource extraction [*Emmerson and Lahn*, 2012], which in turn has led to an increased focus on developing reliable methods to predict the summer sea ice minimum a few months in advance. The Sea Ice Prediction Network solicits predictions of the monthly mean September SIE from the research community beginning in May each year and again in June and July. Different approaches are used to make these forecasts, including coupled ice-ocean/ice-ocean-atmosphere models, statistical models or best guesses based on current conditions. Results from these forecasts have highlighted the difficulty in predicting the September SIE in years when it departs strongly from the long-term trend, with dynamical and statistical models exhibiting similar limitations [*Stroeve et al.,* 2014b, 2015].

While fully coupled models are likely the way forward in seasonal ice forecasting, especially if these models are initialized properly and include essential ice-ocean-atmosphere feedbacks [*Massonnet et al.*, 2015], these models have not provided measureable improvement in skill over simpler statistical models [*Stroeve et al.*, 2014a, 2014b, 2015; *Blanchard-Wrigglesworth et al.*, 2015]. One forecast approach showing a good predictive skill is a statistical model linking modeled melt ponds on sea ice in May to the mean September SIE, explained by the ice-albedo feedback (IAF) [*Schroeder et al.*, 2014]. Satellite observations, on the other hand, find no evidence of skill with Moderate Resolution Imaging Spectroradiometer (MODIS)-derived melt pond fractions in May; instead, the skill increases further into the melt season [*Liu et al.*, 2015]. This is not surprising, since the melt season may start out slowly but then accelerate if a change in weather during summer brings about warmer than normal conditions, enhancing further ice melt. This was the situation in summer 2015, and the Schroeder et al. forecast was biased high by nearly 500,000 km^2.

While melt ponds are important, the timing of when the ice retreats may be a better metric for forecasting the monthly mean September SIE as this information is more readily available from satellite data. The same sort of process holds: earlier ice retreat leads to increased open water area; in turn allowing for more absorption of solar radiation during the time of peak insolation. The increased absorption of solar energy in open water areas accelerates ice melt, further reducing the amount of sea ice at the end of summer. Nevertheless, the prediction of the monthly mean September SIE, which provides an integrated value of total sea ice for the entire Arctic, is of limited value. The timing of when the ice returns to a particular location is an important metric to those operating and living in the Arctic. This is especially relevant for coastal communities, as the presence of sea ice in the fall limits the ability of resupply vessels to reach these northern communities.

In this study we investigate the potential of using information on the timing of sea ice retreat to predict the fall ice advance.

2. Methods

2.1. Sea Ice Data

The data source is the combined Nimbus Scanning Multichannel Microwave Radiometer (SMMR, 1979–1987), the Defense Meteorological Satellite Program (DMSP) Special Sensor Microwave/Imager (SSM/I, 1987–2007), and the Special Sensor Microwave Imager/Sounder (SSMIS, 2007 to present) 25 km gridded sea ice concentration data product from the NASA Team sea ice algorithm [*Cavalieri et al.*, 1996], distributed by the National Snow and Ice Data Center (NSIDC).

2.2. Timing of Retreat and Advance

We apply three sea ice concentration (SIC) thresholds for computing the timing of ice retreat and advance: 15, 30, and 50%. These assignments are made using a sea ice year of 1 March to 28/29 February the following year. For pixels that experience advance after 1 March of the following year, such as in the southern Labrador Sea, this method will give erroneous results. However, within the Arctic basin, this assumption is valid.

The method first records the daily SIC for an entire sea ice year at each pixel. A five-point moving average is then applied to smooth the time series to reduce variability from short-term ice dynamics. Next, the day of the minimum SIC is identified. Lastly, we determine the last retreat day (LRD), the day that the SIC drops to and remains below the SIC threshold, and first advance day (FAD), the first day after the minimum date that SIC is greater than the threshold. All days are measured from 1 March. If a pixel never experiences retreat or advance, it is labeled as NaN.

Our method differs in three key ways from *Stammerjohn et al.* [2012]. First, they define sea ice years from melt season to melt season instead of growth season to growth season. Second, rather than apply a moving average to the daily SIC, they define advance as the day on which SIC first exceeds 15% for at least 5 days. Lastly, for years in which SIC never falls below the concentration threshold, they assign the lower and upper limits for advance and retreat, respectively, whereas we label retreat and advance as NaN for such cases.

Climatological (36 year) mean dates of LRD, FAD, and OWP, together with their long-term trends are derived for each pixel, ignoring NaNs. This results in differences in the number of years included for each pixel when computing a mean and trend (Figure S2): the number of pixels experiencing both retreat and advance decreases toward the pole, with fewer instances for the 15% SIC threshold. In the seasonal ice zones (e.g., Bering, Labrador and Barents seas, Sea of Okhotsk, Baffin, and Hudson bays,), the number of years with retreat/advance is more or less the same for both SIC thresholds. For reference, climatological mean dates of LRD, FAD, and OWP are shown in Figure S3.

2.3. Using Ice Retreat to Forecast Ice Advance

To quantify the relationship between ice retreat and its subsequent advance, we calculate the correlation for each pixel that experiences at least 20 years of retreat and advance over the entire data record. Prior to calculating the Pearson product moment correlation coefficient (r), the time series of retreat and advance for each pixel is detrended. P values are based on an F test. These correlations are also performed over decadal time scales to evaluate how this relationship is changing over time. For decadal correlations, we require at least five valid years. For regional mean analysis, all pixels that record a retreat/advance and exhibit at least

20 retreat/advance cycles are area-weighted averaged across the domain to construct the annual regional mean dates and corresponding trends.

Finally, a linear regression model is used to forecast for each pixel the detrended timing of sea ice advance FAD(y) using the detrended date of retreat LRD(y), such that

$$\mathrm{FAD}(y) = a + b\mathrm{LRD}(y) + \varepsilon(y) \quad (1)$$

where a and b are determined by a least squares procedure by using $N-1$ observations, where N is the number of valid years from 1979 to 2014. Similar to *Schroeder et al.* [2014], we evaluate the forecast skill as $r^2 = 1 - {\sigma_{\mathrm{for}}}^2/{\sigma_{\mathrm{clim}}}^2$, where ${\sigma_{\mathrm{for}}}^2$ is the variance of the forecast error and ${\sigma_{\mathrm{clim}}}^2$ is the variance of the detrended climatology. Next, the omitted year is forecast using this model, and its residual is recorded.

3. Results

3.1. Relationship Between Ice Retreat and Advance

It is useful to first examine trends in LRD, FAD, and the OWP (Figure S4). Sea ice is retreating earlier throughout the Arctic, with the largest trends in the Barents and Kara seas (approximately two or more days earlier each year). The Bering Sea, on the other hand, shows slightly positive trends. This is the only Arctic region with positive SIC trends over the winter/spring months and later surface melt onset [*Stroeve et al.*, 2014a].

Trends are generally similar in magnitude for both SIC thresholds, though regional trends are mostly larger for the 15% SIC threshold (Table S1), which may in part reflect differences in spatial area where valid data exist. Regions with the largest negative LRD trends are also the regions with the largest positive FAD trend: the Barents Sea has the largest negative LRD trend ($\mathrm{Trend}_{\mathrm{Bar,15\%}} = -1.58$; $\mathrm{Trend}_{\mathrm{Bar,50\%}} = -1.31\ \mathrm{d\,y^{-1}}$) and also has one of the largest positive FAD trends ($\mathrm{Trend}_{\mathrm{Bar,15\%}} = +1.77$; $\mathrm{Trend}_{\mathrm{Barents,50\%}} = +1.69\ \mathrm{d\,y^{-1}}$). The only region with larger FAD trends is the Central Arctic Ocean ($+1.82\ \mathrm{d\,y^{-1}}$).

While FAD trends are generally larger than LRD, there are exceptions (e.g., Laptev and Bering seas using either SIC threshold; Hudson and Baffin Bay, the East Greenland and Kara seas using 15% SIC threshold). Note that our trends are considerably smaller than those previously reported by *Stammerjohn et al.* [2012], who evaluated trends from 1979 to 2010. The primary reason for the smaller trends is that we flag years with no retreat as NaN, whereas Stammerjohn et al. identify these pixels as having 365 days of ice coverage. On a per-pixel basis, the latter approach heavily skews statistical calculations but is appropriate for assessing regional changes over time.

The correlation between detrended LRD and detrended FAD using 15% (left) and 50% (right) SIC threshold for the long-term time series is shown in Figure 1. Even after detrending, there is an inverse relationship between the timing of when the ice retreats and when it returns again in the autumn/winter throughout most of the Arctic. However, contrary to what one may have expected given the location of the largest trends in retreat and advance, the strongest inverse correlations ($r < -0.60$) are not found in the Barents Sea but are instead found in Baffin Bay, the Laptev Sea, parts of the Canadian Arctic Archipelago (CAA), and in a few isolated locations in the Kara Sea. The Beaufort and Chukchi seas, as well as the East Siberian and Kara seas, show lower inverse correlations, ranging from $-0.60 < r < -0.40$, and even lower correlations in the seasonal ice zones (e.g., Hudson Bay, Labrador Sea, Barents Sea, and Sea of Okhotsk). Thus, where there is exposure to higher winds, or stronger ocean currents, heat transport or river discharge is where dynamics may dominate over thermodynamics, in turn masking a pixel-by-pixel detection of the IAF. This is not to say that the IAF is not contributing to variability in FAD in these areas, but it is no longer the dominant process governing FAD variability. Furthermore, the correlations are smaller in magnitude than those reported by *Stammerjohn et al.* [2012]. This is primarily a result of the choice to label years without a retreat/advance cycle as NaN.

While we expect an inverse relationship, there are instances where the LRD is positively correlated with the FAD, particularly along the ice edge in the eastern Arctic near Franz Joseph Land and Sevemaya Zemlya. In this region, the seasonality of the OWP for some pixels is highly variable from year to year. For example, around Franz Josef Land in the Nansen Basin, short OWPs (10 days or less) have occurred as early as May and as late as the following February (Figure S5). Late open water occurrences appear to result in part from intrusions of warm water in the mixed layer during winter, leading to ice melt and open water formation [*Ivanov et al.*, 2015]. Therefore, even if some expansion and contraction of the OWP does occur, the change

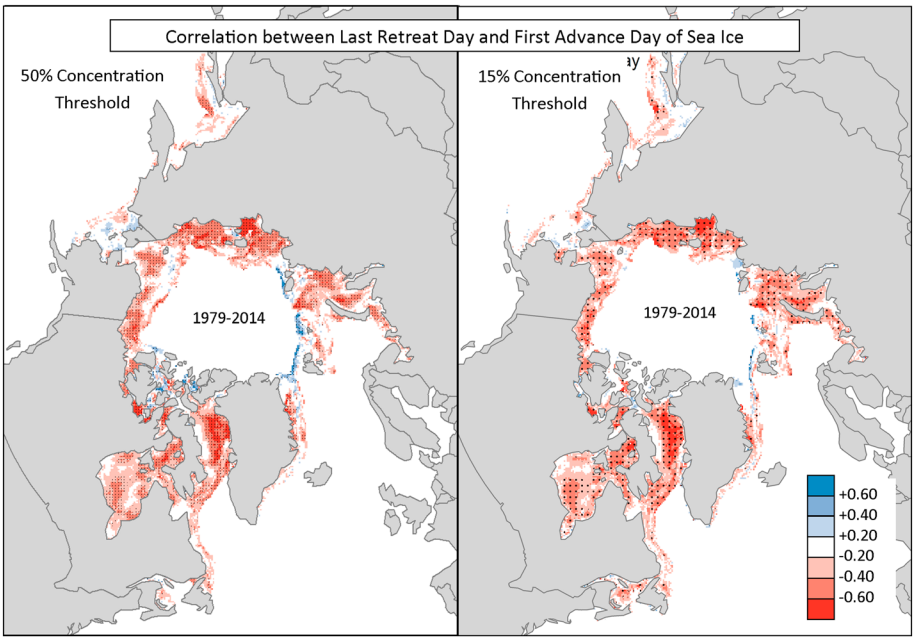

Figure 1. Correlations between detrended 1979–2014 time series of last retreat day and first advance day of sea ice using concentration thresholds of (left) 50% and (right) 15%. Correlations were only calculated for grid cells experiencing at least 20 years with a cycle of sea ice retreat and advance. Stippling is shown for correlations that are statistically significant at the 95% confidence level.

in LRD and FAD is dominated by seasonal shifting of when the OWP occurs. A positive correlation results, meaning that the FAD occurs earlier when the LRD occurs earlier.

The LRD-FAD relationship is generally stronger for the 15% threshold. This makes intuitive sense if the IAF is the dominant process, as there is more open water (85%) to absorb the incoming solar radiation and further warm the ocean mixed layer. At the same time, variability in LRD and FAD could also be a result of wind-driven or ocean-driven ice dynamics. Nevertheless, these results show that even with a 50% open water/ice cover, there is a modest to strong relationship between the timing of when the ice retreats and when it returns.

As a way to graphically illustrate the regional dependence of the LRD-FAD relationship on different SIC thresholds, a regional breakdown of correlations as a function of three thresholds, 15, 30, and 50%, is provided in Figure 2. On a regional basis, the highest inverse correlations occur in Baffin Bay ($r = -0.41$ to -0.37), followed by the East Siberian and Laptev seas ($r = -0.37$ to -0.33). The Beaufort Sea exhibits correlations ranging from $r = -0.37$ to -0.28, and the Kara Sea also shows similar correlations, ranging from $r = -0.34$ to -0.26. Correlations generally decline for a higher SIC threshold. Baffin Bay is an exception, with the highest correlation found for a 30% SIC threshold. Little correlation is seen in the Barents Sea and the other seasonal ice zones except for Hudson Bay.

There is some suggestion that the magnitude of the correlation is increasing with time as open water areas expand in size and duration, allowing the IAF to strengthen (Figure S6). In the overlapping 2000–2009 and 2005–2014 decades, regions of high inverse correlation primarily occur in the Beaufort, Chukchi, East Siberian, and Laptev seas, with the highest inverse correlations generally found offshore. This is similar to what *Stammerjohn et al.* [2012] found in their study (e.g., inner pack ice region), though this was not the case in earlier decades (in our study), where high correlations occurred primarily closest to the coast. On a regional basis, the East Siberian and Laptev seas, as well as the CAA and the Gulf of St. Lawrence have a stronger LRD-FAD relationship since 2000, while the Barents Sea has a weaker relationship with time. This relationship holds regardless of SIC threshold (see Tables S2–S4). Interestingly, the correlation in Baffin Bay is highest during the 1980–1989 decade. This may be more of a reflection of interannual variability in atmospheric conditions, rather than a change in strength of correlation over time. However, there are regions that exhibit persistence of high inverse correlations, especially in the East Siberian and Laptev seas during each decade, suggesting that these may be regions of the Arctic where the IAF dominates and where the timing of ice retreat may be a good predictor for the timing of ice advance.

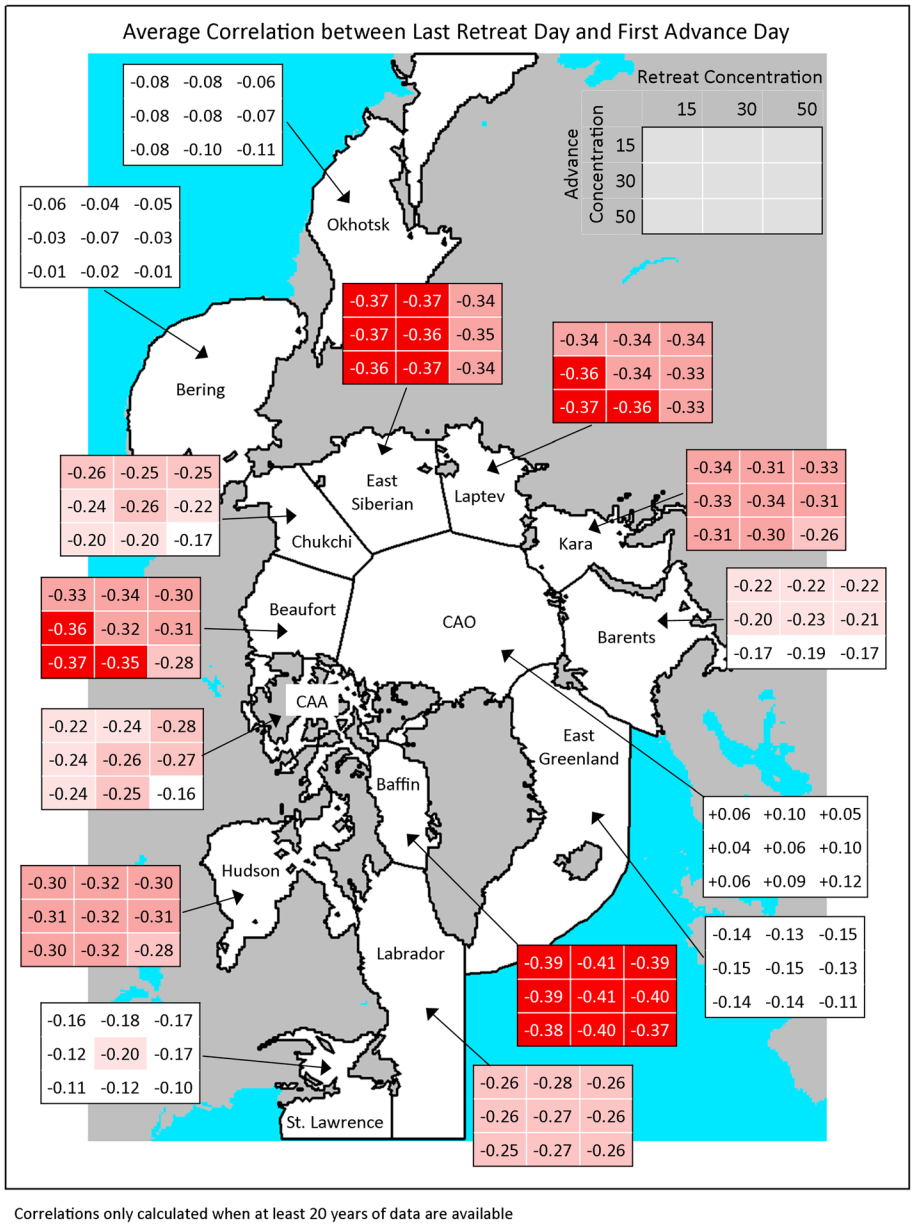

Figure 2. Correlations averaged for individual regions of the Arctic as a function of sea ice concentration threshold (15, 30, or 50%). Correlations are only computed when at least 20 years of data are available. Regional means are computed by first computing the correlation at each pixel and then averaging for the region.

3.2. Using Timing of Retreat to Predict Timing of Advance

Figure 3 shows the average predictive skill (r^2) of predicting the FAD from the LRD. The highest predictive skill occurs in Baffin Bay and the Laptev Sea. Predictive skill is also found in parts of the East Siberian, Beaufort, and Kara seas and the CAA. Elsewhere we do not find the timing of ice retreat to offer much skill in predicting when the ice subsequently returns in autumn/winter.

Regional histograms of predictive skill and residual error are summarized in Figures S7 and S8, respectively, together with the mean predictive skill and mean residual magnitude. Regions of highest potential predictive skill (mean $r^2 \geq 0.20$) are outlined in green and include the Laptev Sea and Baffin Bay. These regions also have small residuals (the mean residual magnitude is 7 and 8 days, respectively) (Figure S8). The Kara, Beaufort, and East Siberian seas, as well as the CAA have a mean predictive skill between $0.15 \leq r^2 \leq 0.20$, whereas all other regions have no predictive skill. The CAO has the largest residual error (mean magnitude of 38 days), followed

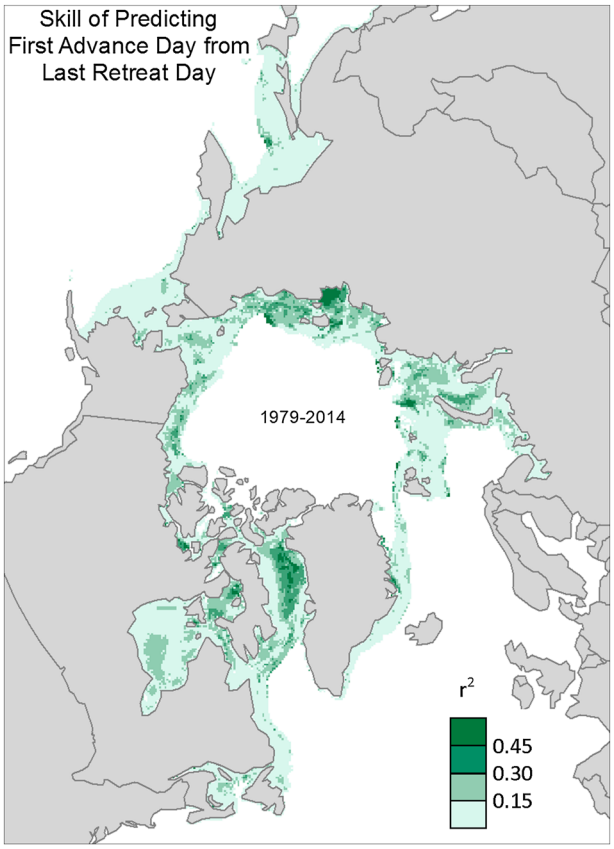

Figure 3. Predictive skill of the linear model FAD(y) = a + b LRD(y), where FAD and LRD are the detrended first advance and last retreat day, respectively, of sea ice in a particular grid cell. The predictive skill is measured as the average r2 value for N models constructed with the above formula, with each model constructed from N-1 years of data, where N is the number of valid years in the period 1979–2014.

by the Barents Sea (24 days) and the East Greenland Sea (24 days). In other regions, the mean residual magnitude is less than 20 days. The combination of predictive skill and residuals allows us to confirm that we are gaining predictive ability in the Laptev Sea and Baffin Bay, but not in other regions, such as Hudson Bay, where residuals are low simply because there are fewer deviations from the trend line.

It is useful to examine a few individual years in more detail and compare the model residual error with the detrended FAD to see when predictions outperform the linear trend. In 1996 the FAD occurred later than expected (relative to the trend line) in the Sea of Okhotsk, the northern Bering Sea, the Chukchi Sea, and the western Kara Sea. FAD was earlier than expected along the coastlines of the eastern Kara, Laptev, East Siberian, and Beaufort seas as well as in most of Baffin Bay (Figure S9, top). Using LRD to predict FAD yields some explanatory power in the southern Chukchi Sea, the Laptev Sea, and Baffin Bay, and the model residuals are smaller than the detrended FAD. Little or no variance is explained in the Sea Okhotsk, the Bering, or the Beaufort seas. In Hudson Bay, the residuals are actually greater than the detrended values.

In 2012, the FAD was later than expected in the Beaufort, Barents, and Kara seas and earlier in the Chukchi and Bering seas (Figure S9, middle). Predicting FAD with LRD helps reduce the detrended variance in several areas, including the Beaufort and Kara seas. However, the residuals are still fairly large in the Kara Sea, and the Chukchi and Bering seas show extreme anomalies. The year 2000 was a fairly normal year for sea ice advance (i.e., close to the trend line), but significant anomalies existed in the Sea of Okhotsk and the Chukchi Sea, where FAD was earlier than expected, and in the Bering Sea, where FAD was much delayed (Figure S9, bottom). As now seems typical for many of the individual cases examined, the LRD is a useful predictor in certain areas, which changes from year to year (e.g., the Beaufort and to some degree the Chukchi Sea in 2000, the Chukchi, Laptev, and Baffin Bay in 1996 and the Beaufort and Kara seas in 2012) and entirely fails to add meaningful information to predictions for regions such as the Sea of Okhotsk, the Bering, or Barents seas. Overall, these examples demonstrate that using LRD to predict FAD is only worthwhile in some regions.

4. Discussion

Several studies have highlighted the importance of the IAF in delaying the formation of ice in autumn/winter [*Stroeve et al.,* 2014a, 2014b; *Steele et al.*, 2008; *Stammerjohn et al.*, 2012]. In this study we use the metric of ice presence rather than freeze-up, which reflects the combined effects of surface freeze-up and ice advection. However, the timing of melt onset plays a role as to when the ice retreats and therefore also when it returns, particularly along most coastal areas, and some fast ice regions, but not in the western Beaufort and northern

Chukchi seas, nor in parts of Baffin Bay (Figure S10). This suggests that dynamics play a larger role (than thermodynamics) in initiating sea ice retreat (and/or advance) in regions of low predictability.

Stammerjohn et al. [2012] note that an earlier sea ice retreat could be attributed to an initial increase in diverging winds (e.g., off-ice winds or cyclonic winds) that open the pack ice and expose open water areas to enhance the IAF. *Boisvert and Stroeve* [2015] argue that increases in specific humidity in May and corresponding downward moisture fluxes cause earlier melt onset, particularly in the Barents and Kara seas, but also to some extent in the Chukchi and Beaufort seas and the CAO. Thus, both atmospheric thermodynamics and dynamic processes associated with synoptic-scale weather patterns can have a large impact on the LRD that would be in addition to the thermodynamic forcing associated with the IAF.

Regarding regional variability in either LRD or FAD, *Stammerjohn et al.* [2012] suggest that decreased winds or ocean currents would favor thermodynamics over dynamics, which in turn would decrease variability in LRD or FAD. Here we find that the LRD exhibits larger interannual variability than the FAD. The largest differences are seen in the Laptev, East Siberian, and Beaufort seas, where the standard deviation is approximately 7 days larger for LRD than for FAD. On the other hand, in the Barents Sea, FAD shows larger interannual variability, though both are quite large (~4 weeks). The East Greenland Sea shows similarly large standard deviations for both the retreat and advance.

Despite some emerging patterns of predictability, prediction in a particular year remains challenging as anomalous late summer circulation patterns vary from year to year and can erode predictability based on this simple feedback model. An additional complication is variability in ocean heat flux, such as variability in the Bering Strait inflow or influx of warm Atlantic water from the Norwegian Sea. This may play a role in predictability in the Chukchi and Barents seas, respectively.

Hard to predict years may additionally be influenced by variability in river discharge, especially for fast ice break-up. Large Arctic rivers provide freshwater to the Arctic Ocean and supply heat to the shelves, which can accelerate fast ice decay [e.g., *Janout et al.,* 2016; *Whitefield et al.*, 2015]. The Lena river discharge peaks in late May/early June when landfast ice is still present and can lead to flooding of the fast ice and early melt out, though a large part of the river discharges under the ice [*Bareiss and Goergen*, 2005]. In the Laptev Sea, increased Lena river discharge combined with earlier sea ice retreat (~2 to 4 d y^{-1}), results in warm summer surface waters, which can be vertically mixed and trapped in the pycnocline [*Janout et al.,* 2016]. River discharge may also contain high values of chromophoric dissolved organic carbon, which absorb solar radiation, leading to enhanced surface warming and lateral ice melt [*Bauch et al.,* 2013].

To evaluate whether river discharge variability may help explain why predictions fail in some years, we examined river discharge data for three rivers, the Lena, Yenisei, and the Ob from R-ArcticNet (http://www.r-arcticnet.sr.unh.edu/v4.0/index.html) and produced seasonal mean discharge rates. Looking at summer, we find no relationship between June, July, August (JJA) discharge and the residual of FAD predicted from LRD in either the Laptev or the Kara seas. During autumn, however, there are modest correlations between SON Lena River discharge and Laptev Sea FAD residuals ($r = +0.45$, SIC = 50%), implying that increased river discharge delays FAD. However, the opposite relationship is found between the SON Yenesei River discharge and the Kara Sea FAD residuals ($r = -0.39$, SIC = 15%).

It is not entirely clear why the relationship differs between these two regions, but it may partly reflect differences in the length of the OWP. The Kara Sea has a longer OWP in which the ocean mixed layer has more time to warm. Thus, warm water from the Lena River may play a larger role in causing the delay in ice advance in the Laptev Sea than the Yenesei River has in the Kara Sea.

Finally, variability in summer river discharge may play a role in LRD, particularly for fast ice. We find positive correlations between the LRD and June river discharge for the Lena River and the Laptev Sea, such that the retreat happens later during years with anomalously high summer discharge (*$r = +0.42$ and $+0.34$ for 15% and 50% SIC, respectively*).

5. Conclusions

An area of high priority for coastal communities is the need for improved predictions of fall ice advance as it is a key constraint for a range of activities and potential hazards (which include exposure of coastlines to fall

storms). Similarly, offshore hydrocarbon exploration activities require a clear definition and prediction of fall ice advance since operations have to cease a little over 1 month prior to the projected ice advance.

This study examines the potential of using a simple statistical model to predict the timing of FAD based on the date that ice retreats. Knowing the LRD increases predictive skill in Baffin Bay, the Laptev and the East Siberian seas even after accounting for the long-term trend in both variables. The Kara and Beaufort seas also have areas with modest increases in predictability, explaining roughly 45% of the variance in the detrended FAD. In other regions (Sea of Okhotsk, Bering and Barents seas, and Hudson Bay), knowing the LRD provides no increase in predictive skill.

In theory, fully coupled models accounting for all aspects of the Arctic system are ideal tools to represent the evolution of sea ice with high fidelity. While idealized model studies suggest a predictability horizon for monthly pan-Arctic SIE of 2 years after initialization, the skill of these models in the "real world" is much lower [*Stroeve et al*., 2014a, 2014b, 2015; *Blanchard-Wrigglesworth et al*., 2015]. Disappointing model results may originate from several limitations of the forecast systems, while it is ultimately possible that inherent predictability in nature may be lower than in climate models. Therefore, our understanding of how the coupled terrestrial, oceanic, and atmospheric systems influence the year-to-year variability of sea ice is largely based on statistical relationships between principal modes of variability of key observations [*Drobot et al*., 2006; *Lindsay et al*., 2008; *Kapsch et al.,* 2013].

Rather than addressing the total Arctic ice extent, we focus on regional scales addressing stakeholder needs. The simple statistical model takes advantage of the inherent predictive power supplied by the seasonal ice-albedo feedback and ocean heat uptake, but we recognize the importance of modulating influences of the summer atmospheric circulation patterns and oceanic heat transport. The importance of this current work is that it sheds light on what sectors of the Arctic are most and least skillful within this simple framework. Future work will look to incorporate information on atmospheric circulation, river discharge, and/or oceanic heat flux.

Acknowledgments
This work was funded under NOAA NA15OAR4310171, NSF PLR 1304246, ONR N000141310434, and the NSF Graduate Research Fellowship Program DGE 1144083. To comply with AGU's data policy, dates of first retreat and last advance are available from ftp://sidads.colorado.edu/pub/projects/SIPN/Retreat_Advance.

References

Bareiss, J., and K. Goergen (2005), Spatial and temporal variability of sea ice in the Laptev Sea: Analysis and review of satellite passive-microwave data and model results, 1997 to 2002, *Global Planet. Change*, *48*, 28–54, doi:10.1016/j.gloplacha.2004.12.004.

Bauch, D., J. A. Hölemann, A. Nikulina, C. Wegner, M. A. Janout, L. A. Timokhov, and H. Kassens (2013), Correlation of river water and local sea-ice melting on the Laptev Sea shelf (Siberian Arctic), *J. Geophys. Res. Oceans*, *118*, 550–561, doi:10.1002/jgrc.20076.

Blanchard-Wrigglesworth, E., R. I. Cullather, W. Wang, J. Zhang, and C. M. Bitz (2015), Model forecast skill and sensitivity to initial conditions in the seasonal Sea Ice Outlook, *Geophys. Res. Lett.*, *42*, 8042–8048, doi:10.1002/2015GL065860.

Boisvert, L. N., and J. C. Stroeve (2015), The Arctic is becoming warmer and wetter as revealed by the Atmospheric Infrared Sounder, *Geophys. Res. Lett.*, *42*, 4439–4446, doi:10.1002/2015GL063775.

Cavalieri, D. J., C. L. Parkinson, P. Gloersen, and H. J. Zwally (1996, updated yearly), Sea ice concentrations from Nimbus-7 SMMR and DMSP SSM/I-SSMIS passive microwave data, version 1. 1 Mar 1979 to 1 Mar 2015. Boulder, Colorado USA. NASA National Snow and Ice Data Center Distributed Active Archive Center, doi:10.5067/8GQ8LZQVL0VL.

Drobot, S. D., J. A. Maslanik, and C. Fowler (2006), A long-range forecast of Arctic summer sea-ice minimum extent, *Geophys. Res. Lett.*, *33*, L10501, doi:10.1029/2006GL026216.

Emmerson, C., and G. Lahn (2012), Arctic opening: Opportunity and risk in the High North, LLoyd's.

Ivanov, V., V. Alexeev, N. Koldunov, I. Repina, A. Sando, L. Smedsrud, and A. Smirnov (2015), Arctic Ocean heat impact on regional ice decay—A suggested positive feedback, *J. Phys. Oceanogr.*, doi:10.1175/JP-D-15-01441.1.

Janout, M., J. Hoelemann, B. Juhls, T. Krumpen, B. Rabe, D. Bauch, C. Wegner, H. Kassens, and L. Timokhov (2016), Episodic warming of near-bottom waters under the Arctic sea ice on the central Laptev Sea Shelf, *Geophys. Res. Lett.*, *43*, 264–272, doi:10.1002/2015GL066565.

Kapsch, M.-L., R. G. Graversen, and M. Tjernstrom (2013), Springtime atmospheric energy transport and the control of Arctic summer sea-ice extent, *Nat. Clim. Change*, *3*, 744–748, doi:10.1038/nclimate1884.

Lindsay, R. W., J. Zhang, A. J. Schweiger, and M. A. Steele, (2008), Seasonal predictions of ice extent in the Arctic Ocean, *J. Geophys. Res.*, *113*, C02023, doi:10.1029/2007JC004259.

Liu, J., M. Song, R. M. Horton and Y. Hu, (2015), Revisiting the potential of melt pond fraction as a predictor for the seasonal Arctic sea ice extent minimum, *Environ. Res. Lett.*, *10*(5), 054017.

Massonnet, F., T. Fichefet, and H. Goosse (2015), Prospects for improved seasonal Arctic ice predictions from multivariate data assimilation, *Ocean Model.*, *88*, doi:10.1016/j.ocemod.2014.12.013.

Perovich, D. K., B. Light, H. Eicken, K. F. Jones, K. Runcimen, and S. V. Nghiem (2007), Increasing solar heating of the Arctic Ocean and adjacent seas, 1979–2005: Attribution and the role of ice-albedo feedback, *Geophys. Res. Lett.*, *34*, L19505, doi:10.1029/2007GL031480.

Schroeder, D., D. Feltham, D. Flocco, and M. Tsamadas (2014), September Arctic sea ice minimum predicted by spring melt pond fraction, *Nat. Clim. Change*, *4*, 353–357.

Serreze, M. C., and J. C. Stroeve (2015), Arctic sea ice trends, variability and implications for seasonal ice forecasting, *Phil. Trans. A.*, *373*, 20140159, doi:10.1098/rsta.2014.0159.

Simmonds, I. (2015), Comparing and contrasting the behavior of Arctic and Antarctic sea ice over the 35 year period 1979–2013, *Ann. Glaciol.*, *56*, 18–28, doi:10.3189/2015A0G69A909.

Stammerjohn, S., R. Massom, D. Rind, and D. Martinson (2012), Regions of rapid sea ice change: An inter-hemispheric seasonal comparison, *Geophys. Res. Lett.*, *39*, L06501, doi:10.1029/2012GL080874.

Steele, M., W. Ermold, and J. Zhang (2008), Arctic Ocean surface warming trends over the past 100 years, *Geophys. Res. Lett.*, *35*, L02614, doi:10.1029/2007GL031651.

Stroeve, J. C., M. C. Serreze, J. E. Kay, M. M. Holland, W. N. Meier, and A. P. Barrett (2012), The Arctic's rapidly shrinking sea ice cover: A research synthesis, *Clim. Change*, doi:10.1007/s10584-011-0101-1.

Stroeve, J. C., T. Markus, L. Boisvert, J. Miller, and A. Barrett (2014a), Changes in Arctic melt season and implications for sea ice loss, *Geophys. Res. Lett*, *41*, 1216–1225, doi:10.1002/2013GL058951.

Stroeve, J. C., L. Hamilton, C. Bitz, and E. Blanchard-Wigglesworth (2014b), Predicting September sea ice: Ensemble skill of the SEARCH sea ice outlook 2008–2013, *Geophys. Res. Lett.*, *41*, 2411–2418, doi:10.1002/2014GL059388.

Stroeve, J. C., E. Blanchard-Wrigglesworth, V. Guemas, S. Howell, F. Massonnet, and S. Tietsche (2015), Developing user-oriented seasonal ice forecasts in a changing Arctic, *Eos Trans. AGU*, *96*, doi:10.1029/2015EO031431.

Whitefield, J., P. Winsor, J. McClelland, and D. Menemenlis (2015), A new river discharge and river temperature climatology data set for the pan-Arctic region, *Ocean Model.*, *88*, 1–15.